3 Biotech (2019) 9:99
https://doi.org/10.1007/s13205-019-1612-0

ORIGINAL ARTICLE

Genome-wide analysis of Chongqing native intersexual goats using next-generation sequencing

Guang-Xin E[1] · Mei-Lan Jin[1] · Yong-Ju Zhao[1] · Xiang-Long Li[2] · Lan-Hui Li[3] · Bai-Gao Yang[1] · Xing-Hai Duan[1] · Yong-Fu Huang[1]

Received: 5 January 2019 / Accepted: 1 February 2019 / Published online: 20 February 2019

Abstract

Sex reversal has been studied extensively in vertebrate species, particularly in domestic goats, because polled intersex syndrome (PIS) has seriously affected their production efficiency. In the present study, we used histopathologically diagnosed cases of PIS to identify correlated genomic regions and variants using representative selection signatures and performed GWAS using Restriction-Site Associated Resequencing DNA. We identified 171 single-nucleotide polymorphisms (SNPs) that may have contributed to this phenotype, and 53 SNPs were determined to be located in coding regions using a general linear model. The transcriptome data sets of differentially expressed genes (DEGs) in the pituitary tissues of intersexual and nonintersexual goats were examined using high-throughput technology. A total of 10,063 DEGs and 337 long noncoding RNAs were identified. The DEGs were clustered into 56 GO categories and determined to be significantly enriched in 53 signaling pathways by KEGG analysis. In addition, according to qPCR results, PSPO2 and FSH were significantly more highly expressed in sexually mature pituitary tissues of intersexual goats compared to healthy controls (nonintersexual). These results demonstrate that certain novel potential genomic regions may be responsible for intersexual goats, and the transcriptome data indicate that the regulation of various physiological systems is involved in intersexual goat development. Therefore, these results provide helpful data for understanding the molecular mechanisms of intersex syndrome in goats.

Keywords RAD · GWAS · RNAseq · Intersexual goat

Introduction

The spontaneous absence of horns (hornless) is a desirable characteristic of many livestock species, because it renders animals easier to handle and less likely to injure each other or their handlers without requiring surgical horn removal; however, the presence of this trait can also lead to female-to-male sex reversal, potentially resulting in intersexual syndrome (Pailhoux et al. 1994). It is well established that the genetic basis of intersex syndrome in goats is associated with the deletion of an 11.7 kb region on chromosome 1 (Pailhoux et al. 2001a; Schibler et al. 2000). While this region contains no known coding sequences, it is known to be involved in the transcriptional regulation of two adjacent genes, PISRT1 and FOXL2, in goats (e.g., Pailhoux et al. 2001b, Crisponi et al. 2001). However, chromosome karyotype structural analysis revealed that, in some cases, many intersexual goats are XX/XY chimeric organisms (e.g., Bongso et al. 1982; Vallenzasca and Galli 1990). These data

E. Guang-Xin, Mei-Lan Jin, and Yong-Ju Zhao have equally contributed to this work.

Electronic supplementary material The online version of this article (https://doi.org/10.1007/s13205-019-1612-0) contains supplementary material, which is available to authorized users.

✉ Yong-Fu Huang
H67738337@swu.edu.cn

[1] College of Animal Science and Technology, Chongqing Key Laboratory of Forage and Herbivore, Chongqing Engineering Research Centre for Herbivores Resource Protection and Utilization, Southwest University, Chongqing 400716, China

[2] College of Animal Science and Technology, Hebei Normal University of Science and Technology, Qinhuangdao 066600, China

[3] College of Animal Science and Technology, Agricultural University of Hebei, Baoding 071001, Hebei, China

suggest a complex regulatory mechanism for intersexual development in goats.

A similar condition, sex reversal syndrome, is frequently reported in humans worldwide (e.g., Pang et al. 2016; Juniarto et al. 2016), and there are a large number of studies exploring its pathogenic molecular mechanisms (Gonen et al. 2018; Harris et al. 2018). However, these studies reveal the complexity of sex development and indicate that multiple mechanisms may coexist. Thus, a multiangle genetic analysis of intersexual goats is necessary to further understand the underlying molecular genetics of sex development and reversal.

In this study, to discover the specific genetic mechanism of Chinese intersexual goats, we comparatively analyzed Chinese intersexual indigenous goats and histopathologically diagnosed using genome-wide sequencing.

Materials and methods

Preparation of animals

We collected four sexually mature (> 1 year of age) intersexual goats (Sample_305, Sample_307, Sample_313, and Sample_315) and five female control individuals (Sample_0308, Sample_1265, Sample_005, Sample_0302, Sample_002; > 1 year of age) with the same bloodlines as those of the previous intersexual goat samples according to a farm survey from Tieshan farm of Chongqing, China (N29°41′20.78″, E105°33′48.95″). Experimental animals were euthanized by sodium pentobarbital injection (0.5–1 mg/kg). The experimental conditions of this study were approved by the Committee on the Ethics of Animal Experiments of Southwest University (no. [2007] 3) and the Animal Protection Law of China.

Histopathological examination

The reproductive organs were excised, and tissue samples from areas similar to the testis, epididymis, ovaries, uterus, and vagina were collected from Sample_0305, Sample_0307, Sample_0313, and Sample_0315. These collected tissue samples were fixed with 10% neutral-buffered formalin and embedded in paraffin. Sections 3 μm in thickness were stained with hematoxylin and eosin (H.E.) for histopathological examination.

Genome-wide correlation analysis and population analysis using RAD resequencing

Genomic DNA from the nine individuals was extracted from blood using a Genomic DNA Purification Kit (Thermo Scientific™). RAD library construction, sample indexing and pooling procedures, and sequencing were performed by Shanghai BIOZERON Biotechnology Co., Ltd. (Shanghai, China) using the Illumina HiSeq2500.

Raw sequencing data were generated by CASAVA v1.8.2. Sickle (Joshi and Fass 2011) with default parameters was used to yield clean data for this study.

The clean reads were aligned to the *Capra hircus* genome (ARS1) using BWA software (Li and Durbin 2009). Single-nucleotide polymorphisms (SNPs) were detected using GATK, and ANNOVAR (see Table 1).

Phylogenetic relationships for all individuals were determined by neighbor-joining phylogenetic analysis (Tamura et al. 2011), principal component analysis (PCA) (Price et al. 2006), and STRUCTURE analysis which were performed using the SNPs. General linear modeling (GLM) was performed using TASSEL v5.2 (Bradbury et al. 2007) to identify the SNPs associated with an intersex phenotype in goats (Wichura 2006).

Genome-wide differential expression analysis of the transcriptome

Pituitary tissues were collected from the eight goats and stored in liquid nitrogen. Total RNA was extracted using TRIzol® reagent according to the manufacturer's protocol (Invitrogen, USA). The RNA quality was determined using a 2100 Bioanalyzer (Agilent, US), and RNA was quantified using the ND-2000 spectrophotometer (NanoDrop Technologies). Equal amounts of RNA from four different individuals were combined into mixed pools [intersexual goat group (IG) and a healthy goat group (HG)]. Ribosomal RNA was removed using the Epicentre Ribo-zero rRNA Removal Kit (Epicentre, Madison, WI, USA). High strand-specific libraries were then generated by NEBNext Ultra Directional RNA Library Prep Kit for Illumina (NEB, Ipswich, MA, USA).

Libraries were sequenced on the Illumina Hiseq 2500 platform by Gene Denovo Technologies (Guangzhou, China) with paired-end reads. Trimming and quality control analysis of raw data were conducted using SeqPrep and Sickle with default parameters to prepare clean reads. The clean reads of each pool were separately aligned to the *C. hircus* genome (ARS1) in orientation mode using Bowtie v2.0.6 software and TopHat v2.0.9. Coding potential and conserved analyses of long noncoding RNAs (lncRNAs) and mRNAs were conducted using CNCI v2, iPfam, and PhyloCSF to identify the final candidate RNAs for further analysis.

Differential expression analysis and functional annotation

The differentially expressed transcripts of coding RNAs and lncRNAs were analyzed separately. Differential expression analysis of the two groups was performed using the DESeq

Table 1 RAD sequencing and family survey classification information of nine Chongqing native goats

Sample_ID	Group	Family	Raw data		Clean data			Sequence composition					SNPs style	
			Reads number	Bases number	Reads number	Base number	Q30%	GC%	A%	T%	C%	G%	Homozygous	Heterozygote
0305	IG	1	8,260,434	1,020,163,599	7,874,176	933,422,886	91.09	45.79	27	27.2	23.19	22.6	446,196	107,550
0308	HG	1	9,485,248	1,166,685,504	9,046,112	1,069,289,831	91.57	45.76	27	27.24	23.17	22.59	471,513	145,102
002	HG	2	2,446,564	302,150,654	2,346,198	272,326,243	88.74	46.53	26.67	26.8	23.56	22.97	107,267	21,623
005	HG	2	5,480,646	679,600,104	5,258,842	625,702,761	90.46	43.19	28.32	28.49	21.9	21.28	362,622	6385
0302	HG	2	9,506,576	1,164,555,560	9,096,744	1,069,050,714	90.93	45.51	27.14	27.35	23.09	22.41	462,378	140,703
0313	IG	2	6,749,178	833,523,483	6,480,032	768,387,819	90.7	45.56	27.12	27.32	23.06	22.5	400,329	102,477
0307	IG	3	5,281,660	652,285,010	5,056,838	595,271,600	89.67	46.15	26.83	27.02	23.36	22.79	318,922	72,591
0315	IG	3	2,868,926	354,312,361	2,746,536	323,708,831	90.57	48.35	25.72	25.93	24.4	23.95	149,629	30,537
1265	HG	3	3,375,784	415,221,432	3,241,186	375,333,469	89	46.94	26.45	26.61	23.74	23.2	191,556	25,718

The family classification is provided by farm managers

IG intersexual goat, *HG* healthy goat

R package (1.10.1). DESeq provides statistical routines for determining the differential expression of digital gene expression data using a model based on the negative binomial distribution. The resulting *P* values were adjusted using Benjamini and Hochberg's approach for controlling the false discovery rate (FDR). Genes with an adjusted *P* value < 0.01 and an absolute log2 value (fold change) > 1 as determined by DESeq were deemed differentially expressed. Differential expression analysis of the two data sets was performed using the EBseq R package. The *P* value was adjusted using the *Q* value. A *Q* value < 0.01 and a |log2 (foldchange)| > 1 were set as the threshold for significant differential expression. GO functional enrichment and KEGG pathway analyses were carried out using Goatools and KOBAS with a Bonferroni-corrected *P* value was less than 0.05.

Quantitative real-time RT-PCR (qPCR)

The samples used in the qPCR analyses were the same as those used in the RNAseq experiment. cDNA was synthesized using the First Strand cDNA Synthesis Kit (GE Healthcare) and 1 mg of total RNA. The primers are shown in Table 2. After a general reverse transcription reaction, PCR analyses were performed in 20 µl amplification reactions containing 10 µl of 2 × SYBR Green PCR Master Mix (Tiangen Biological Technology Co., Ltd, Beijing, China), 20 ng of cDNA, and 0.5 µl (10 mM) of each primer under the following conditions according to the manufacturer's instructions: 95 °C for 10 min for 1 cycle, followed by 40 cycles of 95 °C for 15 s and 60 °C for 45 s (Table 2). The transcripts were quantified using the standard curves with tenfold serial dilutions of cDNA (10^{-7}–10^{-12} g). Melting curves were constructed to verify that only a single PCR product was amplified. Within runs, the samples were assayed in triplicate, with standard deviations of the threshold cycle (CT) values not exceeding 0.5; each qPCR run was repeated at least three times. Negative (without template) reactions were performed within each assay. Significant differences were determined by ANOVA.

Results

Histopathological examinations

In Sample_0305, the seminiferous tubules were lined by Sertoli cells, and no spermatogenic cells were observed in the testis (Fig. 1A-a). Similarly, there were no spermatogenic cells in the duct of the epididymis (Fig. 1A-b). In addition, endometritis with epithelial hyperplasia and inflammatory cell infiltrates were observed in the stroma and gland lumens (Fig. 1A-c). In Sample_0307, we observed dilated epididymis tubules with no sperm, and the uterine glands

Table 2 Information regarding primers used for the amplification of interesting genes using Q-PCR

Gene	Primer name	Sequences (5′–3′)	Tm (℃)
FSHB[A]	FSHB-F	GCGAGACCCAATATCCAGAA	58
	FSHB-R	GGTAGGCAGCTCAAAGCATC	
PENK[A]	PENK-F	GCTTGCACTCTGGAATGTGA	58
	PENK-R	ACCTCCATTTGCCTCTTCCT	
SYNE1[A]	SYNE1-F	TGACAGCCACTTTCAGATGC	58
	SYNE1-R	ACACCAGCTGTTTGGGTTTC	
CDH2[A]	CDH2-F	CCCTCTCCTCTGAACACTCG	60
	CDH2-R	ATGGGAGGGATAACCCAGTC	
TPD52[A]	TPD52-F	AAGCACCTAGCGGAGATCAA	60
	TPD52-R	GAGCCAACAGACGAAAAAGC	
PLP1[A]	PLP1-F	GGCGACTACAAGACCACCAT	60
	PLP1-R	AGGTGGTCCAGGTGTTGAAG	
RERE[A]	RERE-F	AAGACCCGTACTGCATCCAC	60
	RERE-R	CAGTCTTTGGAGGTGGTGGT	
PHF21A[A]	PHF21A-F	CCAAAGCAAGAGGCAAGAAC	60
	PHF21A-R	TCATTTTCAGGGGAGTCAGG	
GBF1[A]	GBF1-F	ACAAAAGCCTCGAGGAGACA	60
	GBF1-R	GGGTTGCTTCCAAACACAGT	
XR_001295696.2[A]	XR_001295696.2-F	ATGAGAGCGAAGTGGAGGAA	60
	XR_001295696.2-R	GTGGTCAAGGCGATCAGAAT	
XR_001919910.1 [A]	XR_001919910.1-F	CCCGTAACAGAAGCTCAAGG	58
	XR_001919910.1-R	GGACATCAAGGTTGGCACTT	
XR_001296733.2[A]	XR_001296733.2-F	ATCCCTGAATCCCTGAATCC	58
	XR_001296733.2-R	ACTCAACTCAGCTCCCCAGA	
XR_001919137.1[A]	XR_001919137.1-F	AATATCACCACGCAGGAAGG	60
	XR_001919137.1-R	AGGGTGGTGTTTCCACAGAG	
XR_309775.3[A]	XR_309775.3-F	GCCATCGCTTATTGAGCTTC	60
	XR_309775.3-R	CCGCAATCTGCTTATCCATT	
PISRT1[B]	PISRT1-F	CTGCTGGGCTGAAGTCATGTC	60
	PISRT1-R	GGCATCAGACTGACCCTGAGTC	
PISRT2 set1[B]	PISRT2 set1-F	TGGAAATCACCTGCCCACTA	60
	PISRT2 set1-R	GCTCATCACAGGACCGTCAG	
PISRT2 set2[B]	PISRT2 set2-F	AGGCTCTCAGATGACACCAAA	60
	PISRT2 set2-R	CCTGAAACTGAGCCAAAGGA	
PFOXIC[B]	PFOXIC-F	CCTACGGGTTGGACGTACGC	60
	PFOXIC-R	AACTGTCCCCCAAAGCCCC	
SOX9[B]	SOX9-F	ACCGCCTTGTCGTTAGACCG	58
	SOX9-R	TCCACGCTCGCTTTGAAGGT	
AMH[B]	AMH-F	ACATACCAGGCCAACAACTG	59
	AMH-R	TGCATCTTTAGCAGCAGCAC	
RSPO1[B]	RSPO1-F	AAGCCGGCGAGTGACTATGC	59
	RSPO1-R	GTCTCTTCCCCTTGATCCCCC	
RSPO2[B]	RSPO2-F	GGTGCAGCCGATGTCAACAG	60
	RSPO2-R	TCCATAGTACCCGGATGGGC	
FSH[B]	FSH-F	ATGGGACTTCAAGGTTGGCA	59
	FSH-R	AAGTGGCATTGTCACTGGCA	
CYP17[B]	CYP17-F	CCCGCTCCTGTGTAGGTGAG	59
	CYP17-R	CTTCCCATCATCCGGGATCT	
CYP19[B]	CYP19-F	AGGTCGGTGCGTTGAGAAGAT	60
	CYP19-R	AGCGCTCGAGGCACTTGTC	

Table 2 (continued)

Gene	Primer name	Sequences (5′–3′)	Tm (℃)
VASA[B]	VASA-F	CGAGGGCTGGATATTGAAAA	60
	VASA-R	TGCCAGTATTTCCACAACGA	
STRA8[B]	STRA8-F	CCTTTTTGAAGATGCCTTCG	60
	STRA8-R	GAGGCTAGATGTGCCTGGAG	
ACTB[B]	ACTB-F	CAGCAAGCAGGAGTACGATGAG	60
	ACTB-R	AAGGGTGTAACGCAGCTAACAGT	
H2AFZ[B]	H2AFZ	GCGTATTACCCCTCGTCACTTG	60
	H2AFZ	CAGCAATTGTAGCCTTGATGAGA	
YWHAZ[B]	YWHAZ-F	GGAGCCCGTAGGTCATCTTG	60
	YWHAZ-R	CTCGAGCCATCTGCTGTTTTT	
DMRT1[B]	DMRT1-F	GAGTTCCCAGTACAGGATGCATT	60
	DMRT1-R	GGGCTGTCCTCAAAAGTGAAGA	
DAZL[B]	DAZL-F	CGTCGGTGGGAAGCATCT	60
	DAZL-R	TCCATCACCTCCAGGTTTCG	
GAPDH	GAPDH-F	AGGCTGGGGCTCACTTGAAG	60
	GAPDH-R	ATGGCGTGGACAGTGGTCAT	

Upper corner A is significant differentially expressed genes and LncRNA from RNAseq, upper corner B is the known sex development-related genes

with endometritis from these collected samples were similar to those of the epididymis or uterine tissues (Fig. 1B). In Sample_0313, a structure resembling the epididymal duct was observed in tissues collected from samples similar to the ovary and uterus. The pathological changes in the testis and epididymis were consistent with those observed in Sample_0305 (Fig. 1C). In addition, we observed endometrial atrophy of the uterus (Fig. 1D). In Sample_0315, structures similar to the ovarian, uterine, and penis glands were observed in tissue collected from samples similar to the ovary, uterus, and penis, respectively (Fig. 1E–G). We observed ovarian atrophy, displayed as a small ovary with prominent stroma, a small corpora lutea, and a similarity to follicular tissue in the ovary (Fig. 1E).

Genome-wide correlation analysis of chromosomal variants related to intersexual goats using high-throughput RAD sequencing

A total of nine RAD accessions from nine individuals (four intersexual goats and five control goats) were constructed and subjected to single-end sequencing. The amount of raw data ranged from 3.02 (Sample_002) to 11.66 Gb (Sample_1265) in each animal (Table 1).

A total of 792,500 SNPs were called from all the samples; 562,965 high-quality SNPs were obtained after filtering (QH of a single SNP ≥ 5 and a missing rate not higher than 5), and the number of SNPs ranged from 128,890 (Sample_002) to 603,081 (Sample_0302). Phylogenetic network (neighbor-joining method) analysis of the nine samples revealed that Sample_005 was inconsistent with the family kinship survey results (Fig. 2). Therefore, we removed Sample_005 from the subsequent analysis, and the RAD data were deposited into GenBank (SRA430625).

After filtering (tolerance of up to four missing samples, minor allele frequency (MAF) ≥ 1/20) the remaining eight samples, 324,904 SNPs were retained, 1527 of which were located in regions encoding genes. According to the PCA plot, phylogenetic clades of the eight individuals were clustered, as shown in Fig. 3a. STRUCTURE analysis was displayed from $K=2$ to $K=5$, and the corresponding maximum-likelihood values of the contribution values of each ancestor type were calculated where $K=3$; because the maximum-likelihood value was the largest, the best K was 3 (Fig. 3b). Therefore, STRUCTURE analysis suggested that these eight animals belonged to three families, which was consistent with the family kinship survey results.

GWAS analysis revealed that 171 SNPs distributed on 28 chromosomes (except chromosomes 22 and 23) had a significant correlation ($P<0.05$) with intersexual features (Fig. 3c). Of these SNPs, 53 were located in gene-coding regions (Table 3).

Identification of differentially expressed transcriptomes in pituitary tissues from intersexual goats and healthy female goats using RNAseq

The sizes of the raw data were 13.75 Gb (HG) and 13.93 Gb (IG). The transcriptome sequencing data from the mixed pools were deposited into the NCBI Sequence database (SRS1497025). In total, 91,652,864 (HG) and 92,852,120 (IG) high-quality clean reads were obtained after rRNA

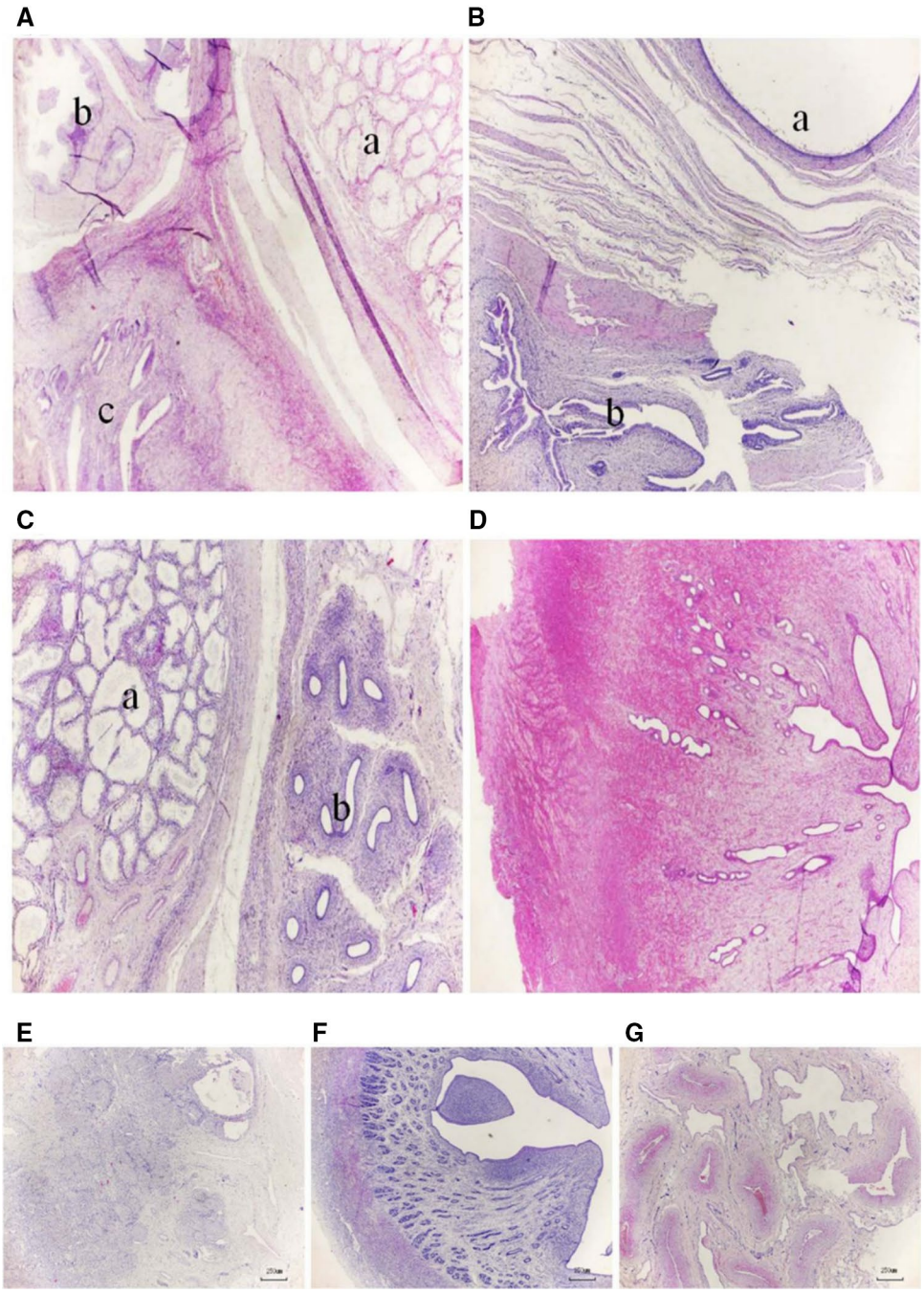

Fig. 1 Histopathological microscopic findings of the intersexual goats' gonads. Histopathological analyses of Sample_0305 (**A**), Sample_0307 (**B**), and Sample_0313 (**C, D**). The parenchyma of Sample_305 goat is distinctly subdivided into a larger right zone of the testis (**A**-a), a small upper left corner zone of the epididymis (**A**-b), and a bottom left corner zone of the uterus (**A**-c); the three zones are separated by a small band of connective tissue. The parenchyma of Sample_0307 goat is distinctly subdivided into the upper right corner zone of the epididymis (**B**-a) and a bottom left corner zone of the uterus (**B**-b); both zones are separated by a small band of connective tissue. The Sample_0313 goat has not only male reproductive organs, such as the testis (**C**-a) and epididymis (**C**-b), but also female reproductive organs, such as the uterus (**D**); the three zones are separated by a small band of connective tissue. Original magnification: **A**–**D** × 25. In addition, microscopic findings of histopathological analysis of ovarian, uterine, and penal tissue from Sample_0315; this goat has not only female reproductive organs, such as ovaries (**E**) and a uterus (**F**), but also male reproductive organs, such as a penis (**G**). Original magnification: **E**–**G** × 40

removal, and the mapping rates were 72.15% and 80.31%, respectively (Table 3). After BLAST analysis against this data set, a total 46,455 transcripts were obtained including 33,157 (71.37%) known isoforms and 6230 novel isoforms (Table 4).

Upon analyzing the digital expression of coding genes in the pituitary tissues of intersexual individuals compared to those in healthy goats, 10,063 coding genes were found to be significantly differentially expressed, including 5477 that were upregulated and 4586 that were downregulated. In addition, 337 lncRNAs were determined to be significantly differentially expressed.

GO analysis of the coding RNAs was performed to classify the functions of DEGs that had hits in the NCBI NR database. These RNAs were summarized under three main GO categories, cellular component, molecular function, and biological process and associated with 56 GO terms (Fig. 4a–c) (Additional File I).

In addition, 294 signaling pathways were annotated. A total of 54 of the 294 KEGG pathways (Additional File II)

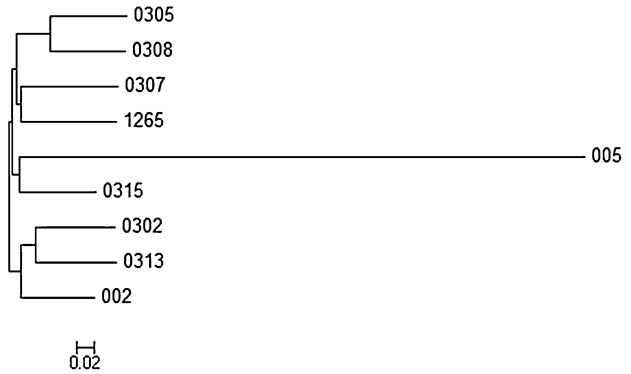

Fig. 2 Phylogenetic relationship assessed of nine goat samples using RAD sequence data

were significantly enriched ($P < 0.05$), and the top 20 pathways are presented in Fig. 4d.

Gene expression profiling and qRT-PCR validation

To verify the accuracy of DEGs from the two mixed pools using RNAseq, we randomly selected 15 significantly differentially expressed mRNAs and lncRNAs identified from the RNAseq for qPCR analysis (Table 4). The qPCR results revealed similar expression profiles, which supported the validity of the RNAseq results (Fig. 5). The result of Q-PCR revealed similar expression profiles, which supported the high credibility of the RNAseq results (Fig. 5). In addition, some sex development-related genes elucidated in the previous intersexual goat research studies (Pannetier et al. 2005; Boulanger et al. 2014; Pailhoux et al. 2001b) were investigated (Fig. 6; Table 4). However, no previously identified genes were significantly ($P < 0.05$) differentially expressed between IG and HG in this study except for the FSH and RSPO2 genes.

Discussion

At necropsy, we found intersexual goats that had both female and male genitalia. Histopathologically, we found testis, epididymis, and uterine tissues in Sample_0305 and Sample_0313, uterine and epididymis tissues in Sample_0307, and ovarian, uterine, and penal tissues in Sample_0315. In addition, we observed pathological changes, such as Sertoli cell-only syndrome, endometritis, and atrophy. These results

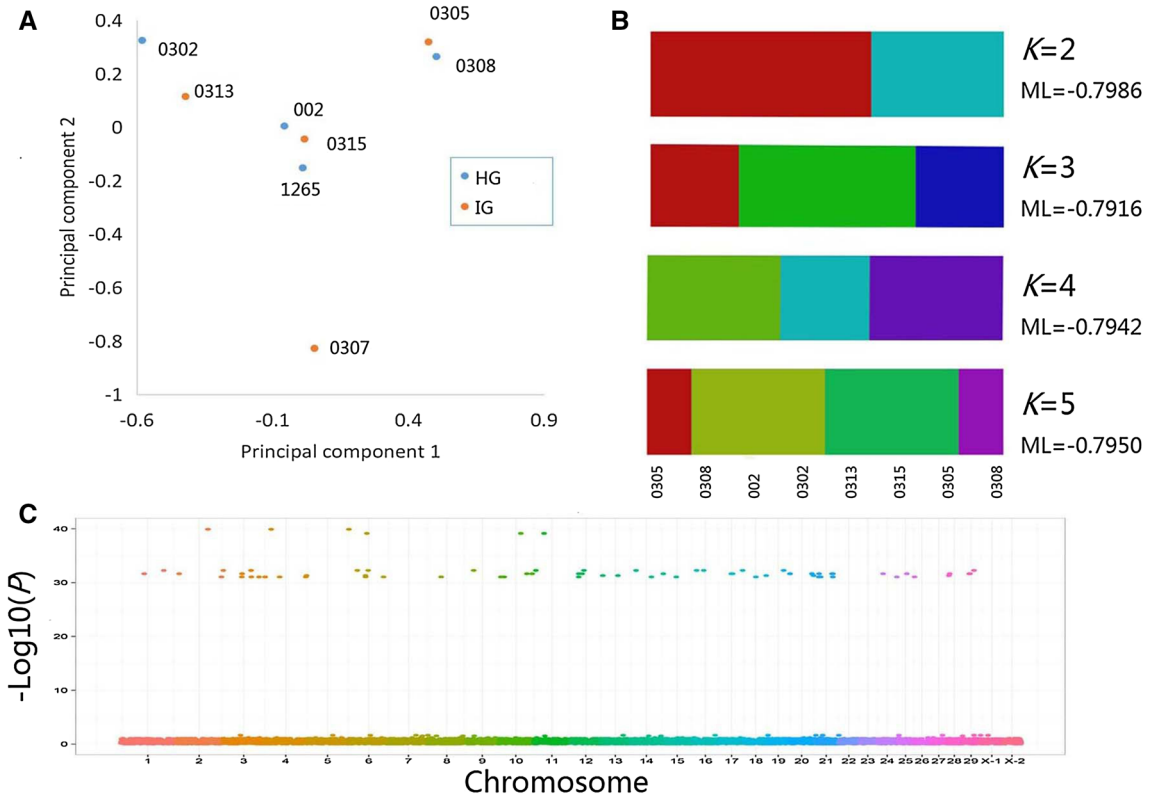

Fig. 3 Genome-wide correlation analysis and phylogenetic analysis of intersexual goats using high-throughput RAD sequencing. **a** Principal component analysis of eight individuals (Sample_005 was removed). **b** Population structure analysis of eight individuals (Sample_005 was removed) using STRUCTURE software. **c** Genome-wide correlation analysis of RAD resequencing data using GLM

Table 3 Information regarding 53 significant SNPs in the gene-coding region

Chromosome	Location	GENE	Coding region	SNP mutation	Amino acid	*P* value
2	91,875,907	LOC102181719	exon1	G92 > A	S31 > N	1.30E−40
2	130,307,289	ADAMTS1	exon2	T999 > C	F333 > F	9.24E−32
3	52,523,643	NRIP1	exon2	C1599 > T	T533 > T	9.24E−32
3	80,271,655	CRYBG3	exon4	A6183 > G	L2061 > L	9.24E−32
3	101,818,509	LOC102173783	exon1	C32 > A	A11 > E	9.24E−32
3	119,201,284	LOC102173783	exon1	G139 > A	A47 > T	9.24E−32
4	117,970,006	CCDC54	exon2	G537 > T	L179 > L	5.20E−32
4	41,178,772	ABI3BP	exon5	G555 > A	K185 > K	9.24E−32
4	115,511,202	IMPG2	exon7	C871 > T	H291 > Y	9.24E−32
6	47,822,577	LOC102174159	exon3	G398 > A	C133 > Y	5.20E−32
6	47,822,774	FBXO40	exon5	C1704 > T	G568 > G	5.20E−32
6	47,822,776	CASR	exon3	T672 > C	I224 > I	9.24E−32
6	99,467,039	LSG1	exon13	G1673 > A	R558 > Q	9.24E−32
8	38,320,631	ATP13A4	exon3	G303 > T	A101 > A	9.24E−32
10	95,292,937	ECT2	exon22	T2295 > C	N765 > N	2.31E−32
10	95,292,988	NCEH1	exon2	C157 > T	L53 > L	2.31E−32
10	5,903,771	TMEM207	exon5	A441 > T	L147 > L	9.24E−32
10	5,903,918	CLDN16	exon4	C333 > T	N111 > N	9.24E−32
10	15,473,437	THPO	exon6	A730 > G	N244 > D	9.24E−32
10	15,473,583	PSMD2	exon5	A504 > G	K168 > K	9.24E−32
10	15,473,584	MCF2L2	exon27	A2966 > G	N989 > S	9.24E−32
12	21,625,793	ACTRT3	exon4	G283 > A	D95 > N	2.31E−32
12	31,342,839	SI	exon7	G823 > A	G275 > R	2.31E−32
12	21,625,778	LRRC34	exon1	A247 > G	T83 > A	9.24E−32
13	3,430,320	GFM1	exon6	A741 > G	A247 > A	5.20E−32
13	46,983,105	SLC33A1	exon1	C564 > T	F188 > F	5.20E−32
14	93,960,898	HPS3	exon2	A504 > G	E168 > E	2.31E−32
14	59,862,310	HPS3	exon4	C910 > G	L304 > V	9.24E−32
15	36,300,093	HPS3	exon2	G393 > A	P131 > P	9.24E−32
17	32,851,977	GYG1	exon6	A729 > G	P243 > P	2.31E−32
17	36,817,815	GYG1	exon6	A721 > G	T241 > A	2.31E−32
18	61,348,015	NME9	exon5	C330 > T	R110 > R	5.20E−32
18	32,110,550	U2SURP	exon10	A783 > G	A261 > A	9.24E−32
20	389,686	PPP2R3A	exon2	G533 > A	R178 > Q	2.31E−32
20	389,698	UMODL1	exon5	G732 > T	S244 > S	2.31E−32
20	62,947,589	TSPEAR	exon7	G1056 > A	T352 > T	2.31E−32
20	67,736,152	LSS	exon5	A543 > T	L181 > L	5.20E−32
21	12,384,062	COL6A5	exon5	A1496 > C	D499 > A	2.31E−32
21	49,213,040	TBC1D5	exon16	A1065 > C	A355 > A	2.31E−32
21	51,940,927	PADI1	exon7	T701 > C	L234 > P	2.31E−32
21	51,941,012	UBR4	exon49	T7398 > C	A2466 > A	2.31E−32
21	11,432,012	COL6A6	exon36	A5964 > C	A1988 > A	9.24E−32
21	17,044,975	CAPN7	exon19	C2103 > T	A701 > A	9.24E−32
21	17,045,057	ANKRD28	exon22	G2352 > A	T784 > T	9.24E−32
21	51,448,755	PP2D1	exon2	G475 > A	E159 > K	9.24E−32
24	17,164,032	ECE1	exon6	C753 > T	N251 > N	2.31E−32
24	56,440,261	HSPG2	exon38	C4788 > T	A1596 > A	9.24E−32
25	23,393,450	MECR	exon6	G859 > C	E287 > Q	2.31E−32
26	2,303,781	LOC108633351	exon11	C1355 > G	A452 > G	9.24E−32
28	7,085,455	LOC102186814	exon12	A1143 > G	T381 > T	2.31E−32
28	5,160,949	LOC102186814	exon12	G1162 > A	D388 > N	5.20E−32

Table 3 (continued)

Chromosome	Location	GENE	Coding region	SNP mutation	Amino acid	*P* value
29	19,035,254	LOC102186814	exon12	T1122 > C	N374 > N	2.31E−32
29	21,205,216	LOC102186814	exon12	C1095 > T	S365 > S	2.31E−32

Table 4 Expression levels of the genes in RNAseq as verified by Q-PCR

Gene_ID	IG_count	HG_count	IG_fpkm	HG_fpkm	log2 (FC)	*P* value	FDR	Significant
XR_001295696.2[A]	64,703	23,368	6849.18	2269.46	− 1.59358	0	0	Yes
XR_001919910.1[A]	224.99	45.06	2.92	0.54	− 2.43494	1.96E−24	2.16E−22	Yes
XR_001296733.2[A]	228.26	57.33	10.2	2.35	− 2.11784	5.20E−20	4.15E−18	Yes
XR_001919137.1[A]	0	35.74	0.001	1.84	10.84549	7.54E−12	2.68E−10	Yes
XR_309775.3[A]	3	14	0.2	0.86	2.104337	0.007564	0.035817	Yes
FSHB[A]	4907.44	32135.85	236.04	1418.1	2.586856	0	0	Yes
PENK[A]	5020.75	65.2	167.44	1.99	− 6.39473	0	0	Yes
SYNE1[A]	178.55	493.86	0.34	0.85	1.321928	3.23E−28	7.62E−27	Yes
CDH2[A]	205	492	3.41	7.5	1.137119	4.40E−22	7.34E−21	Yes
GTF2I[A]	26.91	0	0.45	0.001	− 8.81378	7.59E−09	4.16E−08	Yes
TPD52[A]	115.86	61.12	4.56	2.21	− 1.04499	4.29E−06	1.65E−05	Yes
PLP1[A]	23.47	830.52	0.39	12.79	5.035398	5.6E−190	3.69E−187	Yes
RERE[A]	382.64	843.28	2.52	5.09	1.014242	3.15E−30	8.24E−29	Yes
PHF21A[A]	29.83	70.36	0.38	0.83	1.127112	0.000422	0.001168	Yes
GBF1[A]	57.2	1.05	0.46	0.01	− 5.52356	1.15E−16	1.31E−15	Yes
PISRT1[B]	0	0	0.001	0.001	0	1	1	No test
PISRT2[B]	0	0	0.001	0.001	0	1	1	No test
PFOXIC[B]	0	0	0.001	0.001	0	1	1	No test
SOX9[B]	56	77	0.71	0.9	0.342106	0.226168	0.319874	No
AMH[B]	1	0	0.02	0.001	− 4.32193	1	1	No
RSPO1[B]	2.85	0	0.13	0.001	− 7.02237	0.250037	0.343799	No
RSPO2[B]	113	26	0.42	1.68	2	2.05E−12	1.62E−11	Yes
FSH[B]	7367.15	886.56	80.63	614.71	2.930517	0	0	Yes
CYP17[B]	0	0	0.001	0.001	0	1	1	No test
CYP19[B]	0	0	0.001	0.001	0	1	1	No test
STRA8[B]	1	2	0.05	0.09	0.847997	1	1	No
ACTB[B]	3123.06	4348.5	140.65	179.68	0.35332	9.51E−19	1.26E−17	No
YWHAZ[B]	2866.15	3770.55	48.86	58.98	0.271572	9.54E−11	6.46E−10	No
DMRT1[B]	1	0	0.02	0.001	− 4.32193	1	1	No
DAZL[B]	0	0	0.001	0.001	0	1	1	No test

Upper corner A is significant differentially expressed genes and LncRNA from RNAseq, and upper corner B is known sex development-related genes

are consistent with those of the previous reports (Poth et al. 2010; Szatkowska et al. 2015).

We performed a genome-wide scan of four intersexual individuals and four controls that were collected from the same farm. Phylogenetic analyses based on PCA and STRU CTURE confirmed that both the genetic background and family clustering of the eight goats corresponded to their previously known kinship. This experimental design avoids false-positive effects caused by individual genetic differences and, thus, allows the identification of valuable mutations in fewer pedigree populations. These two goat groups provided a great opportunity to investigate the intersexual syndrome mechanism of goats with a smaller sample size.

By analyzing the autosome genomic resequencing data set using GLA, we identified 35 SNPs located in gene-coding regions that showed a significant correlation ($P < 0.05$) with this phenotype. Most of the genes were associated with various biological functions. For example, some mitochondrial function regulation-related genes, such as MECR, cause a distinct human disorder of the mitochondrial fatty

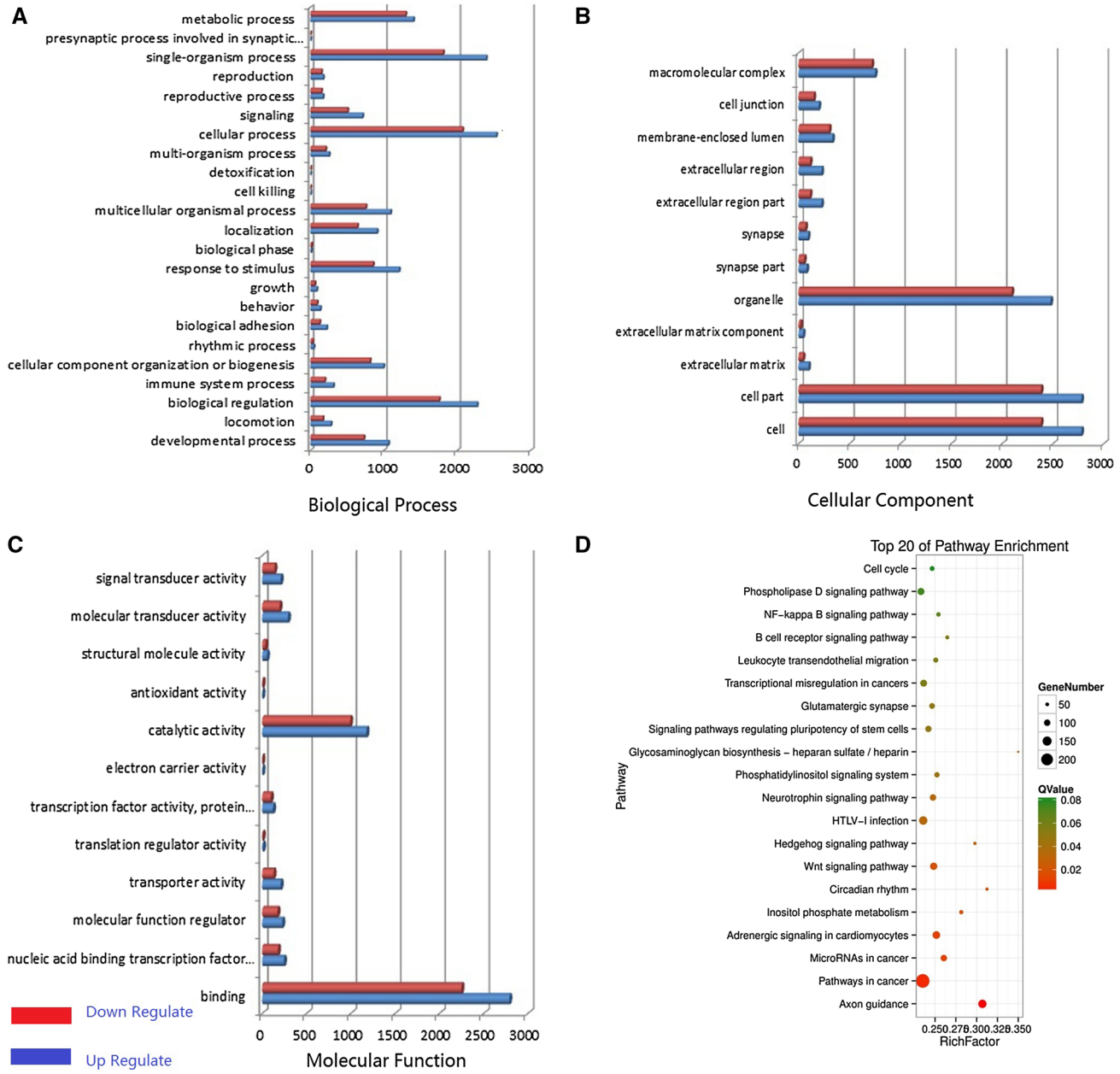

Fig. 4 Differential expression analysis of pituitary tissues from HG and IG using high-throughput technology. **a**–**c** Differentially expressed gene distributions of gene ontology (GO) categories (level 2) of HG and IG mixed pools in goats. GO functional annotations are summarized into three main categories: biological process, cellular component, and molecular function. *x*-axis in panel **a**–**c** is the number of gene. **d** Top 20 enriched pathways of coding genes differentially expressed between HG and IG

acid synthesis pathway (Parl et al. 2013; Chen et al. 2008), and NRIP1 is a factor known to be involved in mitochondrial dysfunction and energy expenditure (Lapierre et al. 2015). Furthermore, some SNPs related to the immune system and emotional regulation were identified, such as ADAMTS1, which plays an important regulatory role in tumor and autoimmune diseases (Silva et al. 2016; Hirohata et al. 2017), and SLC33A1, which has been shown to be involved in mood regulation (Hullinger et al. 2016).

In a previous report, deletion of 11.7 kb on chromosome 1 was identified to contribute to PIS in goats (Pailhoux et al. 2001a). However, in our GWAS, no significant correlating candidate sites were observed near this chromosomal region. On one hand, this outcome could result from a lack of effective variant sites generated by low-density genome resequencing technology, as well as fewer samples. On the other hand, this finding could indicate that different genetic mechanisms can result in intersexual goats. In brief, a wide

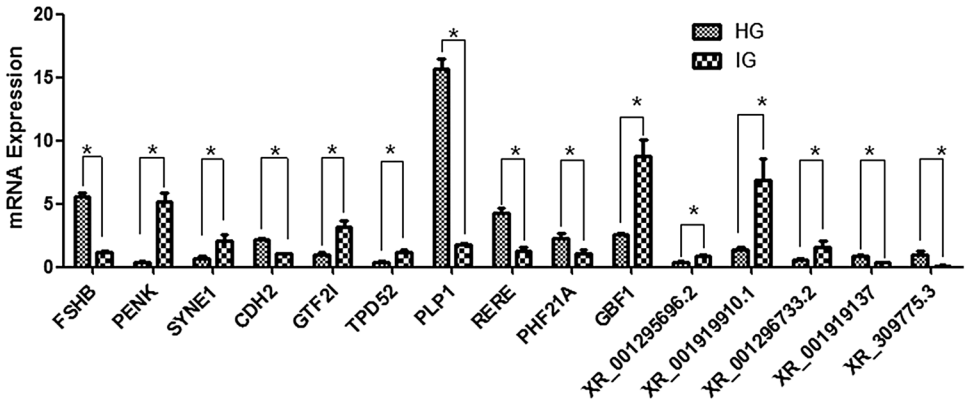

Fig. 5 Real-time PCR validation of significantly differentially expressed genes and lncRNAs in pituitary tissues from HG and IG. The abundance of target genes was normalized relative to that of the GAPDH gene. Bars in each panel represent the mean ± standard error (sample number = 4 and 3 parallel repetitions per sample); * indicates significant differential expression ($P < 0.05$)

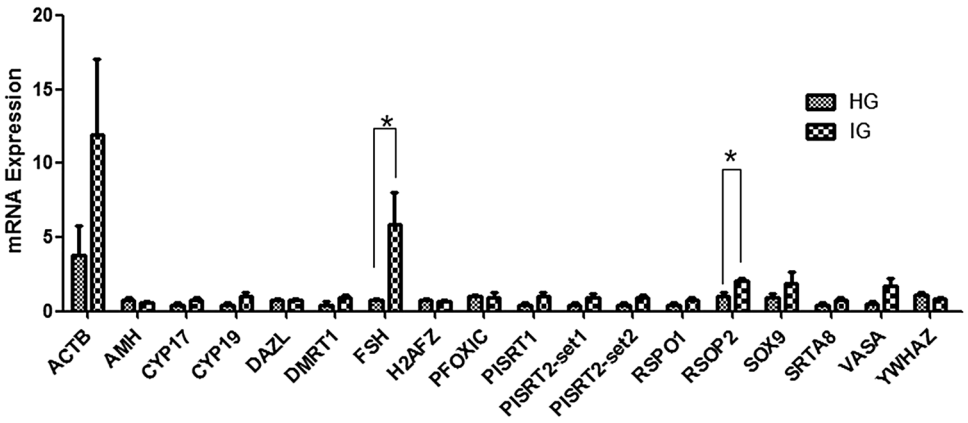

Fig. 6 Validation of the expression levels of 18 known sex development-related gene sets in pituitary tissues from HG and IG using Q-PCR; * indicates significant differential expression ($P < 0.05$)

range of genes which participate in various biological functions have been identified helpful in explaining the physiology and development of intersexual goats.

In exploring the molecular genetic features of intersexual goats, we were not only evaluated genomic DNA but also assessed genes at the transcriptome level. Interestingly, in the coding gene analysis, a number of genes were annotated in molecular pathways, such as the phospholipase D signaling, axon guidance, progesterone-mediated oocyte maturation, and oxytocin signaling pathways. In particular, some signaling pathways that are widely involved in the regulation of various biological functions were also identified, such as the FoxO and cAMP pathways.

The FoxO pathway plays a role in follicular development and female reproductive disorders (Sheridan et al. 2015; Huang et al. 2016). In addition, the MAPK pathway is involved in the development of some tissues; for example, it promotes the osteoblastic differentiation of ligament fibroblasts (Chen et al. 2016). Recent studies have indicated that polymorphisms in the MAPK anginal pathway factor, MAPK1, and CREB1 genes have significant associations with anxiety disorder comorbidities (Antypa et al. 2016).

Coincidentally, some neurological development-related pathways were also found including the dopaminergic synapse and neurotrophin signaling pathways, which may be associated with abnormal behavior and depression in intersexual goats (Chen et al. 2016). In addition, two hormone-related signaling pathways, the oxytocin signaling pathway and the adrenergic signaling pathway in cardiomyocytes, were identified in this study, and many studies have already suggested that these hormones play important roles in sex development disorders (Fisher et al. 2016; Zhang 2014).

In addition, some interesting pathways were not significantly enriched in this study but may still be related to the development of intersexual traits. Eighteen endocrine system-related signaling pathways, including the progesterone-mediated oocyte maturation, estrogen signaling, and GnRH and PPAR signaling pathways, were identified, which infers that the abnormal development of sexual organs may have an inalienable relationship with hormones in intersexual animals.

During the last 50 years, numerous reports on dirty vulvar tissue and extensive urinary tract infections among intersexual goats with extremely low immunity have appeared (Zhang 2014). According to the results of the current study, 24 signaling pathways belonging to immune diseases and the immune system were discovered; this finding could explain the above pathological manifestations.

Currently, as an emerging genetic marker, lncRNAs have been studied in numerous in-depth human medicine studies,

such as those on neurodegenerative diseases and tumorigenesis (Maoz et al. 2017; Yang et al. 2018). In this study, 337 differentially expressed lncRNAs were found in IG and HG, which indicates that lncRNAs may be involved in the regulation of development in intersexual goats. Therefore, a large number of coding RNAs and lncRNAs with significantly differential expression were detected between two mixed pools using RNAseq, indicating that the appearance of intersex syndrome is due to the regulation of various physiological systems. In addition, among the 15 mRNAs and lncRNAs whose expression was verified, 93.33% were consistent with the RNAseq results, except SYNE1. This finding shows that the RNAseq results were highly credible.

Finally, we herein identified the mRNA differential expression profiles of some sex-revised and developmentally relative candidate genes between IG and HG individuals using qPCR. For example, as previously described, the expression levels of AMH, CYP19, SOX3, and WNT4 in the gonads and internal genital organs of intersexual goats in different developmental periods can be increased or decreased depending on the number of days after coitus (Pailhoux et al. 2002). However, in this study, except for PSPO2 and FSH, most of these genes were not significantly differentially expressed in sexually mature pituitary tissue. This result could be caused by the timing and tissue specificity of gene expression.

Interestingly, PSPO2 is known to play an important role in ovarian follicular growth (Bouilly et al. 2017) and is involved in some developmentally related signaling pathways (Dong et al. 2017; Ilmer et al. 2015). In addition, FSH genetic variations have been associated with genital lesions and infertility in males (André et al. 2018; Tamburino et al. 2017) as well as with ovary and various female gonad developmental processes (Wei et al. 2018). Therefore, the significantly higher expression levels of these two genes in IG pituitary tissues are insufficient to explain the molecular mechanism of intersexual goats, but they may be involved in the maintenance of the physiological phenotype and biological regulation of intersexual goats.

Conclusion

The results of this study are helpful for comprehensively understanding the genetic mechanism of intersexual goats in China, and the development of novel biomarkers can support pathological identification. Intersexual goats can serve as a sex reversal animal model, and the molecular genetic results from this study can provide a new understanding of sex reversal and development.

Acknowledgements This work was supported by Fundamental Research Funds for the Central Universities (XDJK2018B014), National Natural Science Foundation of China (no. 31172195), the Characteristic Germplasm Resources Population Selection and Innovation on Mutton Sheeps and Goats (no. 2015BAD03B05), and Chongqing Research Program of Basic Research and Frontier Technology (cstc2018jcyjAX0153).

Compliance with ethical standards

Conflict of interest The authors declare no conflict of interest.

References

André GM, Martins Trevisan C, Pedruzzi IN, Fernandes RFM, Oliveira R, Christofolini DM, Bianco B, Barbosa CP (2018) The impact of FSHR gene polymorphisms Ala307Thr and Asn680Ser in the endometriosis development. DNA Cell Biol 37(6):584–591. https://doi.org/10.1089/dna.2017.4093

Antypa N, Souery D, Tomasini M, Albani D, Fusco F, Mendlewicz J, Serretti A (2016) Clinical and genetic factors associated with suicide in mood disorder patients. Eur Arch Psychiatry Clin Neurosci 266(2):181–193

Bongso TA, Thavalingam M, Mukherjee TK: Thavalingam, Mukherjee TK (1982) Intersexuality associated with XX/XY mosaicism in a horned goat. Cytogenet Cell Genet 34(4):315–319

Bouilly J, Beau I, Barraud S, Bernard V, Delemer B, Young J, Binart N (2017) R-spondin2, a novel target of NOBOX: identification of variants in a cohort of women with primary ovarian insufficiency. J Ovarian Res 10(1):51. https://doi.org/10.1186/s13048-017-0345-0

Boulanger L, Pannetier M, Gall L, Allais-Bonnet A, Elzaiat M, Le Bourhis D, Daniel N, Richard C, Cotinot C, Ghyselinck NB, Pailhoux E (2014) FOXL2 is a female sex-determining gene in the goat. Curr Biol 24(4):404–408

Bradbury PJ, Zhang Z, Kroon DE, Casstevens TM, Ramdoss Y, Buckler ES (2007) TASSEL: software for association mapping of complex traits in diverse samples. Bioinformatics 23:2633–2635

Chen ZJ, Pudas R, Sharma S, Smart OS, Juffer AH, Hiltunen JK, Wierenga RK, Haapalainen AM (2008) Structural enzymological studies of 2-enoyl thioester reductase of the human mitochondrial FAS II pathway: new insights into its substrate recognition properties. J Mol Biol 379(4):830–844. https://doi.org/10.1016/j.jmb.2008.04.041

Chen D, Liu Y, Yang H, Chen D, Zhang X, Fermandes JC, Chen Y (2016) Connexin 43 promotes ossification of the posterior longitudinal ligament through activation of the ERK1/2 and p38 MAPK pathways. Cell Tissue Res 363(3):765–773. https://doi.org/10.1007/s00441-015-2277-6

Crisponi L, Deiana M, Loi A, Chiappe F, Uda M, Amati P, Bisceglia L, Zelante L, Nagaraja R, Porcu S, Ristaldi MS, Marzella R, Rocchi M, Nicolino M, Lienhardt-Roussie A, Nivelon A, Verloes A, Schlessinger D, Gasparini P, Bonneau D, Cao A, Pilia G (2001) The putative forkhead transcription factor FOXL2 is mutated in blepharophimosis/ptosis/epicanthus inversus syndrome. Nat Genet 27(2):159–166

Dong X, Liao W, Zhang L, Tu X, Hu J, Chen T, Dai X, Xiong Y, Liang W, Ding C, Liu R, Dai J, Wang O, Lu L, Lu X (2017) RSPO2 suppresses colorectal cancer metastasis by counteracting the Wnt5a/Fzd7-driven noncanonical Wnt pathway. Cancer Lett 402:153–165

Fisher AD, Ristori J, Fanni E, Castellini G, Forti G, Maggi M (2016) Gender identity, gender assignment and reassignment in individuals with disorders of sex development: a major of dilemma. J Endocrinol Investig 39(11):1207–1224

Gonen N, Futtner CR, Wood S, Garcia-Moreno SA, Salamone IM, Samson SC, Sekido R, Poulat F, Maatouk DM, Lovell-Badge R (2018) Sex reversal following deletion of a single distal enhancer of Sox9. Science 360(6396):1469–1473. https://doi.org/10.1126/science.aas9408

Harris A, Siggers P, Corrochano S, Warr N, Sagar D, Grimes DT, Suzuki M, Burdine RD, Cong F, Koo BK, Clevers H, Stévant I, Nef S, Wells S, Brauner R, Ben Rhouma B, Belguith N, Eozenou C, Bignon-Topalovic J, Bashamboo A, McElreavey K, Greenfield A (2018) ZNRF3 functions in mammalian sex determination by inhibiting canonical WNT signaling. Proc Natl Acad Sci USA 115(21):5474–5479. https://doi.org/10.1073/pnas.1801223115

Hirohata S, Inagaki J, Ohtsuki T (2017) Diverse functions of a disintegrin and metalloproteinase with thrombospondin motif-1. Yakugaku Zasshi 137(7):811–814. https://doi.org/10.1248/yakushi.16-00236-4

Huang P, Zhou Z, Shi F, Shao G, Wang R, Wang J, Wang K, Ding W (2016) Effects of the IGF-1/PTEN/Akt/FoxO signaling pathway on male reproduction in rats subjected to water immersion and restraint stress. Mol Med Rep 14(6):5116–5124

Hullinger R, Li M, Wang J, Peng Y, Dowell JA, Bomba-Warczak E, Mitchell HA, Burger C, Chapman ER, Denu JM, Li L, Puglielli L (2016) Increased expression of AT-1/SLC33A1 causes an autistic-like phenotype in mice by affecting dendritic branching and spine formation. J Exp Med 213(7):1267–1284

Ilmer M, Boiles AR, Regel I, Yokoi K, Michalski CW, Wistuba II, Rodriguez J, Alt E, Vykoukal J (2015) RSPO2 enhances canonical Wnt signaling to confer stemness-associated traits to susceptible pancreatic cancer cells. Cancer Res 75(9):1883–1896

Joshi NA, Fass JN (2011) Sickle: a sliding-window, adaptive, quality-based trimming tool for FastQ files (Version 1.33). https://github.com/najoshi/sickle

Juniarto AZ, van der Zwan YG, Santosa A, Ariani MD, Eggers S, Hersmus R, Themmen AP, Bruggenwirth HT, Wolffenbuttel KP, Sinclair A, White S, Looijenga LH, de Jong FH, Faradz SM, Drop SL (2016) Hormonal evaluation in relation to phenotype and genotype in 286 patients with a disorder of sex development from Indonesia. Clin Endocrinol (Oxf) 85(2):247–257. https://doi.org/10.1111/cen.13051

Lapierre M, Docquier A, Castet-Nicolas A, Gitenay D, Jalaguier S, Teyssier C, Cavaillès V (2015) The emerging role of the transcriptional coregulator RIP140 in solid tumors. Biochim Biophys Acta 1856(1):144–150. https://doi.org/10.1016/j.bbcan.2015.06.006

Li H, Durbin R (2009) Fast and accurate short read alignment with burrows-wheeler transform. Bioinformatics 25:1754–1760

Maoz R, Garfinkel BP, Soreq H (2017) Alzheimer's disease and ncRNAs. Adv Exp Med Biol 978:337–361. https://doi.org/10.1007/978-3-319-53889-1_18 **(Review)**

Pailhoux E, Cribiu EP, Chaffaux S, Darre R, Fellous M, Cotinot C (1994) Molecular analysis of 60, XX pseudohermaphrodite polled goats for the presence of SRY and ZFY genes. J Reprod Fertil 100:491–496

Pailhoux E, Vigier B, Chaffaux S, Servel N, Taourit S, Furet JP, Fellous M, Grosclaude F, Cribiu EP, Cotinot C, Vaiman D (2001a) A 11.7-kb deletion triggers intersexuality and polledness in goats. Nat Genet 29(4):453–458

Pailhoux E, Vigier B, Vaiman D, Schibler L, Vaiman A, Cribiu E, Nezer C, Georges M, Sundrstrom J, Pelliniemi LJ, Fellous M, Cotinol C (2001b) Contribution of domestic animals to the identification of new genes involved in sex determination. J Exp Zool 290:700–708

Pailhoux E, Vigier B, Vaiman D, Servel N, Chaffaux S, Cribiu EP, Cotinot C (2002) Ontogenesis of female-to-male sex-reversal in XX polled goats. Dev Dyn 224(1):39–50

Pang XL, Long W, Li J, Yang J (2016) 45, XO/47, XXX/46, XX male sex reversal syndrome. A case report. J Reprod Med 61(9–10):510–512

Pannetier M, Renault L, Jolivet G, Cotinot C, Pailhoux E (2005) Ovarian-specific expression of a new gene regulated by the goat PIS region and transcribed by a FOXL2 bidirectional promoter. Genomics 85(6):715–726

Parl A, Mitchell SL, Clay HB, Reiss S, Li Z, Murdock DG (2013) The mitochondrial fatty acid synthesis (mtFASII) pathway is capable of mediating nuclear-mitochondrial cross talk through the PPAR system of transcriptional activation. Biochem Biophys Res Commun 441(2):418–424. https://doi.org/10.1016/j.bbrc.2013.10.072

Poth T, Breuer W, Walter B, Hecht W, Hermanns W (2010) Disorders of sex development in the dog—adoption of a new nomenclature and reclassification of reported cases. Anim Reprod Sci 121(3–4):197–207

Price AL, Patterson NJ, Plenge RM, Weinblatt ME, Shadick NA, Reich D (2006) Principal components analysis corrects for stratification in genome-wide association studies. Nat Genet 38(8):904–909

Schibler L, Cribiu EP, Oustry-Vaiman A, Furet JP, Vaiman D (2000) Fine mapping suggests that the goat polled intersex syndrome and the human blepharophimosis ptosis epicanthus syndrome map to a 100-kb homologous region. Genome Res 10:311–318

Sheridan R, Belludi C, Khoury J, Stanek J, Handwerger S (2015) FOXO1 expression in villous trophoblast of preeclampsia and fetal growth restriction placentas. Histol Histopathol 30(2):213–222

Silva SV, Lima MA, Cella N, Jaeger RG, Freitas VM (2016) ADAMTS-1 is found in the nuclei of normal and tumoral breast cells. PLoS One 11(10):e0165061

Szatkowska I, Zaborski D, Proskura WS, Tabor S (2015) Polledness intersex syndrome in goats—molecular and histological aspects. Turk J Vet Anim Sci 38(6):612–617

Tamburino L, La Vignera S, Tomaselli V, Condorelli RA, Cannarella R, Mongioì LM, Calogero AE (2017) The– 29G/A FSH receptor gene polymorphism is associated with higher FSH and LH levels in normozoospermic men. J Assist Reprod Genet 34(10):1289–1294

Tamura K, Peterson D, Peterson N, Stecher G, Nei M, Kumar S (2011) MEGA5: molecular evolutionary genetics analysis using maximum likelihood, evolutionary distance, and maximum parsimony methods. Mol Biol Evol 28(10):2731–2739. https://doi.org/10.1093/molbev/msr121 **(PMID: 21546353)**

Vallenzasca C, Galli A (1990) Cytogenetical and histopathologic study of two cases of polled goats. Andrologia 22(3):289–290

Wei S, Shen X, Lai L, Liang H, Deng Y, Gong Z, Che T (2018) FSH receptor binding inhibitor impacts K-Ras and c-Myc of ovarian cancer and signal pathway. Oncotarget 9(32):22498–22508. https://doi.org/10.18632/oncotarget.25139

Wichura MJ (2006) The coordinate-free approach to linear models. Cambridge series in statistical and probabilistic mathematics. Cambridge University Press, Cambridge, pp 14–199 **(ISBN 978-0-521-86842-6. MR 2283455)**

Yang YX, Wei L, Zhang YJ, Hayano T, Piñeiro Pereda MDP, Nakaoka H, Li Q, Barragán Mallofret I, Lu YZ, Tamagnone L, Inoue I, Li X, Luo JY, Zheng K, You H (2018) Long non-coding RNA p10247, high expressed in breast cancer (lncRNA-BCHE), is correlated with metastasis. Clin Exp Metastasis. https://doi.org/10.1007/s10585-018-9901-2

Zhang Y (2014) Study on PIS region, PISRT1 and FoxL2 genes in polled intersex dairy goat (D). Agricultural University of Hebei, Shijiazhuang **(in Chinese)**